Research Article

Estimation of interaction parameters of electrolyte NRTL model based on NaCN and Na$_2$CO$_3$ solubility in water–ethanol mixed solvent and process simulation for separation of NaCN/Na$_2$CO$_3$

Kang-Il Kim[1,2] · Jong-Hyok Ri[3] · Se-Ung Kim[2,4] · Il-Hyok Kim[5]

Abstract

The solubility of NaCN and Na$_2$CO$_3$ in the water–ethanol mixture was determined through experiments. Also the polynomial fit was used to lead to the relationship between the solubility of NaCN/Na$_2$CO$_3$ and the solvent composition. In the meantime, the solvent molecular-electrolyte pair interaction parameters of electrolyte NRTL (eNRTL) model were estimated by using the data regression function of Aspen Plus software from solubility data of NaCN and Na$_2$CO$_3$ in water–ethanol mixed solvent. The process simulation for separation and purification of NaCN and Na$_2$CO$_3$ in water–ethanol mixed solvent was carried out by using Aspen Plus software. During the simulation, electrolyte equilibrium system in water–ethanol mixed solvent was observed by using eNRTL model property method, and the influence of several factors on the separation efficiency of NaCN was examined.

Keywords Solubility · Electrolyte NRTL model · Mixed solvent · NaCN · Separation · Process simulation

1 Introduction

High purity NaCN is widely used in many fields including electroplating, precious metal smelting, catalyst industry and the demand for high purity NaCN is getting higher [1–5]. The crude NaCN usually obtained by the solid phase synthesis method contains sodium salts such as Na$_2$CO$_3$ and sodium formate (NaHCOO).

Many studies have been already carried out to produce pure NaCN from low-grade NaCN [6, 7]. One effective method to obtain pure electrolyte from a crude is by using the solubility difference between NaCN and other impurities in a suitable solvent [8, 9]. Solvents which dissolve NaCN but not for other impurities are already introduced.

For example, it was known that methanol or ethanol could be used to dissolve NaCN and then the solution was evaporated to dryness to recover the purified form. Anhydrous ammonia is also well known solvent and a process for obtaining the pure cyanide by dissolving crude using anhydrous ammonia under pressure followed by evaporation of ammonia is also proposed. Due to not so high solubility of NaCN in anhydrous alcohol, anhydrous methanol or anhydrous ethanol consume a large amount of solvent in the dissolution step and a great deal of energy in the evaporation step.

Solubility and productivity of NaCN in solvent had been increased by using water–ethanol mixed solvent. The first thing in designing the purification process of NaCN in a

✉ Kang-Il Kim, kgi1983@mail.dlut.edu.cn; Jong-Hyok Ri, ri_jonghyok@163.com; Se-Ung Kim, chem@mail.dlut.edu.cn; Il-Hyok Kim, ilhyokkim@163.com | [1]Institute of Advanced Science, Kim Il Sung University, Pyongyang 999093, Democratic People's Republic of Korea. [2]Department of Management & Economic, Dalian University of Technology, Dalian 116023, People's Republic of China. [3]Department of Chemistry, Kim Il Sung University, Pyongyang 999093, Democratic People's Republic of Korea. [4]Department of Applied Chemical Engineering, Kim Chaek University of Technology, Pyongyang 950003, Democratic People's Republic of Korea. [5]Department of Metallurgical Engineering, Kim Chaek University of Technology, Pyongyang 950003, Democratic People's Republic of Korea.

water–ethanol mixed solvent is to determine the solubility of the materials in the mixed solvent. In this paper, solubility data for NaCN and Na_2CO_3 in water–ethanol mixed solvent were measured at different temperatures. These data have been used to simulate the process for separating NaCN and Na_2CO_3 in a water–ethanol mixed solvent.

The eNRTL model is widely used for phase equilibrium calculations in mixed solvent electrolyte systems [9–11]. This model was proposed by Chen [12] as an extension of the NRTL model of Renon and Prausnitz [13]. The eNRTL model was modified by Chen and Song [14] and recently supplemented by Bollas et al. [15]. The eNRTL model divides non-ideal contribution into a short range binary contribution and a long range electrostatic contribution. Activity coefficients are calculated based on asymmetry, where the reference state of the solvent is pure solution and the reference state of the solute is the infinitely diluted state in water. It is very important to precisely determine the interaction parameters of the solvent molecule–electrolyte pair when simulating electrolyte equilibria in mixed solvents using eNRTL models. Many parameters for eNRTL model have been stored in the databanks provided by Aspen Plus software. However, some parameters must be determined by experiment [16, 17]. In this paper, eNRTL model parameters were estimated from the solubility data of NaCN and Na_2CO_3 in water–ethanol mixed solvent. The estimated parameters were also used to simulate the process. Then, the process for separation of NaCN and Na_2CO_3 in water–ethanol mixed solvent was simulated by using Aspen Plus software.

Aspen Plus is a steady-state process simulator for predicting the behavior of a process or group of unit operations through existing relationships between them. Aspen Plus software process simulation is used in computer-aided design, process optimization (e.g., improving production and process efficiency, minimizing operational costs and emission of waste that may be contaminant, improving energy efficiency, etc.), solving operational problems, and so on [18–20]. In this paper, optimization of the process for the separation of NaCN and Na_2CO_3 mixtures in a water–ethanol mixed solvent was carried out.

2 Determination of solubility of NaCN and Na_2CO_3 in water–ethanol mixed solvents

2.1 Experimental

2.1.1 Chemicals and instrumentation

Ethanol was supplied by Merck and used without further purification (mass fraction purity >0.99). The purity of ethanol was checked by gas chromatography (GC). In this study, deionized and redistilled water was used. NaCN (>99 wt%) and anhydrous Na_2CO_3 (99 wt%) were purchased from Wako Pure Chemicals Industries, Ltd. (Osaka, Japan). In addition, 0.1000 mol/L Silver nitrate titration solution, 10% aqueous solution of potassium iodide and 25 wt% aqueous ammonia solution are used. All of these substances were of analytical grade. Aqueous solutions were prepared just before use by dissolving the reagent in ultrapure water.

As instrument, a magnetic stirrer (IKA RO10), electronic balance (Sartorius BT25S, ±0.000001 kg), constant temperature bath (FDLRTS-0A, ±0.01 °C), Vacuum drying oven (HD-E804-30B) were used in this study. Phase identification of solid phase was performed with X-ray diffraction analysis (XRD, Rigaku SmartLab, CuKα radiation from rotating anode X-ray tube, 1.5406 Å).

2.1.2 Experimental methods

First, a solid sample (NaCN and Na_2CO_3) was excessively added to pure water and various concentrations of a water–ethanol mixed solvent, and the mixture was thoroughly stirred by a magnetic stirrer. Next, the sample was placed in a constant temperature bath and allowed to stand at a constant temperature for 24 h or longer to reach an equilibrium state.

When the solid–liquid equilibrium is sufficiently reached, 1.00 mL of the supernatant is sampled from the sample, and the mass of the solution is weighed. The content of Na_2CO_3 in the solution was determined by evaporating the solution at 150 °C and weighing the remaining solid sample. The content of NaCN was determined by coordination titration using a 0.1000 mol/L silver nitrate solution as a titration solution and a 10 wt% potassium iodide aqueous solution as an indicator.

The solubility of NaCN and Na_2CO_3 at the respective temperatures and solvent compositions was determined from the mass of the solution and the amount of solid sample dissolved therein.

On the other hand, the remaining sample was separated by filtration to obtain a solid component. The crystal structure of the solid in solid–liquid equilibrium state was analyzed by powder X-ray diffraction analysis. The XRD patterns were taken in the angular range 2θ = 20°–60° with a scanning speed of 2°/min and step angle of 0.02°. Qualitative phase analysis has been performed using MDI JADE 9.0 software. All structural data for each of the phase are according to ICDD.

Table 1 Solid equilibrium data of NaCN–H$_2$O binary system

No.	T (°C)	S (g/100 g solvent)	Solid phase
1	0	29.90 ± 1.47	NaCN·2H$_2$O
2	15	34.20 ± 1.82	NaCN·2H$_2$O
3	28	40.00 ± 2.02	NaCN·2H$_2$O
4	35	48.50 ± 3.11	NaCN·2H$_2$O
5	40	56.80 ± 2.74	NaCN
6	45	63.70 ± 4.43	NaCN
7	50	68.10 ± 3.98	NaCN

2.2 Results and discussions

The solubility of the NaCN electrolyte in the NaCN–H$_2$O binary system at different temperatures are shown in Table 1. Where T is the temperature of the solution and S is the solubility of the salt in the liquid phase.

According to the X-ray analysis results, there are the two solid phases, NaCN·2H$_2$O and NaCN, in the NaCN–H$_2$O binary system: NaCN·2H$_2$O in the low temperature, NaCN in the high temperature. All diffraction peaks of NaCN and NaCN·2H$_2$O in the NaCN–H$_2$O two-dimensional system are same with ICDD reference code 75-0872, 29-1206 respectively, and the space group of these two phases are belong to Immm of orthorhombic and P21/c of monoclinic respectively. Figure 1 shows the XRD patterns considering the change in the solid phase according to the temperature.

The relationship between the temperature and solubility of NaCN in pure water was regressed using Eq. (1) in Origin 8.1, and the following result was obtained.

$$S = A + BT + CT^2 + DT^3 \tag{1}$$

A = 30.21327, B = −0.15778, C = 0.0231, D = −8.5487·10^{-5}, δ = 0.97982.
Here, $\delta = \sum[(S_{cal} - S_{exp})^2/N]^{1/2}$, N is the number of test points.

On the other hand, the solubility measurement data for NaCN–C$_2$H$_5$OH–H$_2$O ternary system at each temperature is shown in Table 2. Where C is the content of ethanol in the solvent and S is the solubility of NaCN in solution.

NaCN–C$_2$H$_5$OH–H$_2$O ternary system, as in the NaCN–H$_2$O binary system, there are two solid phases of NaCN·2H$_2$O and NaCN present, the higher the temperature and ethanol content, the higher the NaCN content.

The results of Eq. (2) regression of the solubility relationship of NaCN according to the solvent composition are shown in Table 3.

$$S = A + Bw_{ROH} + Cw_{ROH}^2 + Dw_{ROH}^3 \tag{2}$$
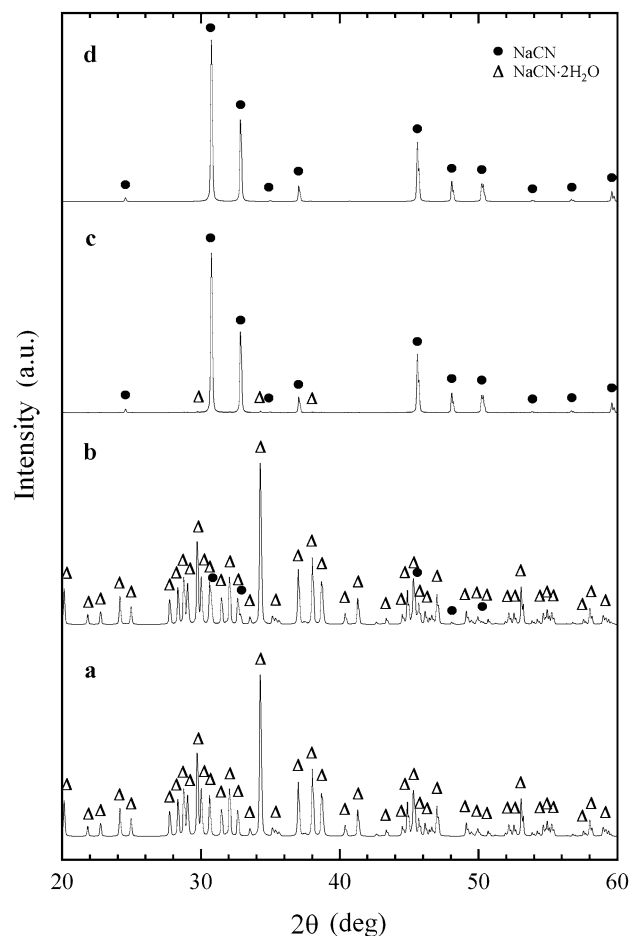
Fig. 1 XRD patterns for solid phases in NaCN–H$_2$O binary system at temperature of 28 °C in **a**, 35 °C in **b**, 40 °C in **c** and 45 °C in **d**

In the equation, w_{ROH} is the mass fraction of ethanol in the mixed solvent.

Next, the solubility measurement data for Na$_2$CO$_3$–C$_2$H$_5$OH–H$_2$O ternary system at each temperature is shown in Table 4. The liquid-phase equilibrium data for the Na$_2$CO$_3$–H$_2$O binary system have not been reported here because they have already been reported in the prior literatures. Where C is the content of ethanol in the solvent and S is the solubility of Na$_2$CO$_3$ in solution.

Figure 2 shows X-ray patterns in accordance with temperature in the NaCN–C$_2$H$_5$OH–H$_2$O ternary system of the content of 64.9% ethanol. In the Na$_2$CO$_3$–C$_2$H$_5$OH–H$_2$O ternary system, there may be exist at least one of the three solid phases, Na$_2$CO$_3$·10H$_2$O, Na$_2$CO$_3$·7H$_2$O, and Na$_2$CO$_3$·H$_2$O, depending on the conditions of temperature and the changes in ethanol content. According to the X-ray diffraction analysis, all diffraction peaks of these phases are same with ICDD reference code 75-7991, 70-2148 and 09-3809 respectively, and the space group of these three

Table 2 Solid–liquid equilibrium data of NaCN–C₂H₅OH–H₂O ternary system

T (°C)	C (wt%)	S (g/100 g solvent)	Solid phase
27	0	40.40 ± 3.62	NaCN·2H₂O
	8.10	35.60 ± 2.88	NaCN·2H₂O
	25.4	30.50 ± 1.92	NaCN·2H₂O
	44.8	19.90 ± 1.01	NaCN·2H₂O
	64.9	8.95 ± 0.64	NaCN·2H₂O
	76.0	4.67 ± 0.26	NaCN·2H₂O + NaCN
	87.7	1.87 ± 0.09	NaCN·2H₂O + NaCN
	99.7	0.80 ± 0.03	NaCN
31	0	44.10 ± 3.34	NaCN·2H₂O
	8.10	38.50 ± 2.56	NaCN·2H₂O
	25.4	32.20 ± 1.87	NaCN·2H₂O
	44.8	24.00 ± 1.81	NaCN·2H₂O
	64.9	9.11 ± 0.69	NaCN·2H₂O
	76.0	5.01 ± 0.27	NaCN·2H₂O + NaCN
	87.7	2.08 ± 0.12	NaCN·2H₂O + NaCN
	99.7	0.91 ± 0.07	NaCN
35	0	48.50 ± 3.99	NaCN·2H₂O
	8.10	42.80 ± 2.78	NaCN·2H₂O
	25.4	34.90 ± 2.21	NaCN·2H₂O
	44.8	24.60 ± 1.90	NaCN·2H₂O
	64.9	10.25 ± 0.76	NaCN·2H₂O + NaCN
	76.0	5.15 ± 0.33	NaCN·2H₂O + NaCN
	87.7	2.12 ± 0.14	NaCN
	99.7	0.97 ± 0.08	NaCN
40	0	56.80 ± 4.31	NaCN
	8.10	48.90 ± 3.02	NaCN
	25.4	37.30 ± 2.21	NaCN
	44.8	26.80 ± 1.74	NaCN
	64.9	9.31 ± 0.67	NaCN
	76.0	5.21 ± 0.35	NaCN
	87.7	2.39 ± 0.19	NaCN
	99.7	1.26 ± 0.10	NaCN
45	0	63.70 ± 4.68	NaCN
	8.10	53.00 ± 3.36	NaCN
	25.4	43.90 ± 2.87	NaCN
	44.8	27.00 ± 1.85	NaCN
	64.9	11.60 ± 0.94	NaCN
	76.0	5.60 ± 0.31	NaCN
	87.7	2.54 ± 0.16	NaCN
	99.7	1.40 ± 0.09	NaCN
50	0	68.10 ± 4.72	NaCN
	8.10	59.60 ± 3.45	NaCN
	25.4	47.90 ± 2.89	NaCN
	44.8	30.10 ± 1.47	NaCN
	64.9	12.60 ± 0.65	NaCN
	76.0	5.73 ± 0.29	NaCN
	87.7	3.77 ± 0.20	NaCN
	99.7	2.87 ± 0.12	NaCN

phases are belong to C1c1 of monoclinic, Pbca and P21ab of orthorhombic respectively.

The results of Eq. (2) regression of the solubility relationship of Na_2CO_3 according to the solvent composition are shown in Table 5.

3 Estimation of interaction parameters between solvent molecule–electrolyte pair interaction of eNRTL model

eNRTL model is a multidimensional model for calculating electrolyte activity coefficient and not only can be expressed in the water-soluble electrolyte system but also can be expressed in the mixed electrolyte system over the entire electrolyte concentration range by using the various interaction parameters.

In this model, the asymmetric Pitzer–Debye–Huckel model and the Born equation are used to denote contributions due to remote ion–ion interactions, and the NRTL model is used to indicate contribution due to local interaction (Figs. 3 and 4).

In general, the parameters for the eNRTL model include:

(a) The dielectric constant of a pure component in a non-aqueous solvent.
(b) Born radius of ion species.
(c) NRTL parameters for molecule–molecule, molecule–electrolyte, electrolyte–electrolyte pair.

In the non-aqueous solvent, the dielectric constant of the pure component and the born radius of the ionic species are required only in the mixed solvent electrolyte system. All forms of eNRTL parameters are consist of two non-random factors α and an energy parameter τ.

Many parameters are included in the eNRTL model parameter databank provided by Aspen. First, the databank contains most of the binary parameters (NRTLs) for molecular–molecule interactions. There is also a certain amount of data on the non-coincidence factor (GMELCN) and the energy parameter (GMELCC, GMELCD, GMELCE) for the molecule–electrolyte pair and the electrolyte–electrolyte pair.

However, the values of some of these parameters are not given and in most cases they should be estimated through experiments. In particular, the Aspen Plus databank does not include molecular–electrolyte interaction parameters we are trying to estimate, except H_2O–(Na^+, CO_3^{2-}).

Therefore, we have estimated the interaction parameters between solvent molecules (water or ethanol)–electrolytes (NaCN or Na_2CO_3) pairs based on solubility data

Table 3 Parameter values standard deviations (SD) of the solubility relationship Eq. (2) of NaCN according to mixed solvent composition

T (°C)	A	SD_A	B	SD_B	C	SD_C	D	SD_D	δ
27	39.495	1.011	−22.986	0.896	−74.226	0.966	58.506	1.223	0.99603
31	42.726	0.984	−21.905	0.937	−85.448	1.009	65.356	0.964	0.98899
35	47.418	0.977	−32.099	1.110	−79.176	0.921	64.656	1.088	0.99517
40	55.545	1.103	−58.078	1.304	−53.515	0.987	57.192	1.141	0.99082
45	61.863	0.991	−65.473	0.815	−58.790	0.884	63.752	0.993	0.99258
50	66.951	0.889	−59.252	0.779	−95.950	0.901	91.386	0.989	0.99616

of NaCN and Na_2CO_3 in a water–ethanol mixed solvent experimentally determined previously.

In this study, the data regression function provided by Aspen Plus (v8.4) was used to regress the solvent molecule–electrolyte pair interaction parameters of the eNRTL model from solubility experimental data.

To do this, we selected the electrolyte process standard simulation model in the Aspen Plus (v8.4) software and set the data regression method as the run mode. We then defined the required components in the [Components] folder of the [Properties] guide list and used the [Elec wizard] technique to define the various chemical reactions that can occur in the electrolyte system and the resulting species. In addition, the ELECNRTL model is set up by the physical property method, and the model parameters provided in the Aspen Plus databank are searched and defined. Next, in the [Data] folder of the [Properties], the experimental data for the solid–liquid phase equilibrium in each electrolyte system (H_2O–NaCN, H_2O–C_2H_5OH–NaCN and H_2O–C_2H_5OH–Na_2CO_3) were entered. Then, regression was performed after setting the initial value, the upper limit value, and the lower limit value of the molecular-electrolyte pair interaction parameters in the [Regression] folder.

The interaction parameters of the molecule–electrolyte pairs that are regressed using the Aspen Plus software are shown in Tables 6, 7, and 8, respectively.

The solubility of NaCN and Na_2CO_3 in water and water–ethanol mixture that simulated by using the molecular–electrolyte interaction parameters obtained by regression of the solubility data was compared with experimental data. The results are shown in Figs. 5 and 6, respectively.

As can be seen from Figs. 5 and 6, the simulation results are comparable to the experimental results. Therefore, the previously estimated solvent molecule–electrolyte pair interaction parameters can be used to simulate the NaCN and Na_2CO_3 separation processes in a water–ethanol mixed solvent.

4 Process simulation for separation of NaCN and Na_2CO_3 mixture by using water–ethanol mixed solvent

4.1 Establishment of process model

4.1.1 Create process diagram

The process of separating materials using solubility differences in mixed solvents generally consists of dissolving, filtering, evaporating and drying the raw material mixture.

The Aspen Plus process diagram for separating NaCN and Na_2CO_3 mixture in water–ethanol mixed solvent is shown in Fig. 7. As shown in Fig. 7, the major unit operating models used in the process simulation are Flash2 (gas–liquid separator), CFuge (crystallizer), and Dryer (dryer). In the process diagram, the SOLUTION model (Flash2) simulates the electrolyte equilibrium process when the raw materials (NaCN and Na_2CO_3 mixture) are dissolved in a water–ethanol mixed solvent. The SEPARATE model (CFuge) simulates the centrifugation process of Na_2CO_3 precipitates that are not dissolved in mixed solvents. The EVAPOR model (Crystallizer) simulates the process of obtaining NaCN crystals by evaporating and concentrating the NaCN solution. The DRYER model simulates the process of completely removing the moisture contained in NaCN crystals from the crystallizer.

Definition of component First, NaCN and Na_2CO_3, H_2O, C_2H_5OH are defined as general components. Next, since NaCN, Na_2CO_3, and H_2O exist in the electrolyte form, they use the Electrolyte Wizard function provided by Aspen Plus to define electrolyte dissociation equilibrium and all other components obtained during the salt formation process. The results are shown in Table 9.

Table 4 Solid–liquid equilibrium data of Na_2CO_3–C_2H_5OH–H_2O ternary system

T (°C)	C (wt%)	S (g/100 g solvent)	Solid components
25	0	31.90 ± 1.91	$Na_2CO_3 \cdot 10H_2O$
	8.10	29.80 ± 1.49	$Na_2CO_3 \cdot 10H_2O$
	16.6	20.40 ± 0.81	$Na_2CO_3 \cdot 10H_2O$
	25.4	15.026 ± 0.751	$Na_2CO_3 \cdot 10H_2O$
	44.8	1.386 ± 0.083	$Na_2CO_3 \cdot 10H_2O$
	64.9	0.150 ± 0.009	$Na_2CO_3 \cdot H_2O$
	70.4	0.0605 ± 0.0030	$Na_2CO_3 \cdot H_2O$
	76.0	0.0410 ± 0.0024	$Na_2CO_3 \cdot H_2O$
30	0	38.90 ± 2.32	$Na_2CO_3 \cdot 10H_2O$
	8.10	33.20 ± 1.89	$Na_2CO_3 \cdot 10H_2O$
	16.6	25.80 ± 1.31	$Na_2CO_3 \cdot 10H_2O$
	25.4	15.667 ± 0.939	$Na_2CO_3 \cdot 10H_2O$
	44.8	1.401 ± 0.076	$Na_2CO_3 \cdot 10H_2O$
	64.9	0.161 ± 0.008	$Na_2CO_3 \cdot H_2O$
	70.4	0.0910 ± 0.0055	$Na_2CO_3 \cdot H_2O$
	76.0	0.0601 ± 0.0032	$Na_2CO_3 \cdot H_2O$
35	0	46.50 ± 2.81	$Na_2CO_3 \cdot 7H_2O$
	8.10	38.30 ± 1.93	$Na_2CO_3 \cdot 7H_2O$
	16.6	28.20 ± 1.70	$Na_2CO_3 \cdot 7H_2O$
	25.4	16.195 ± 0.81	$Na_2CO_3 \cdot 7H_2O$
	44.8	1.472 ± 0.087	$Na_2CO_3 \cdot 7H_2O$
	64.9	0.189 ± 0.011	$Na_2CO_3 \cdot H_2O$
	70.4	0.142 ± 0.007	$Na_2CO_3 \cdot H_2O$
	76.0	0.0632 ± 0.0038	$Na_2CO_3 \cdot H_2O$
40	0	48.40 ± 2.79	$Na_2CO_3 \cdot H_2O$
	8.10	36.20 ± 2.10	$Na_2CO_3 \cdot H_2O$
	16.6	30.10 ± 1.51	$Na_2CO_3 \cdot H_2O$
	25.4	16.812 ± 0.796	$Na_2CO_3 \cdot H_2O$
	44.8	1.517 ± 0.071	$Na_2CO_3 \cdot H_2O$
	64.9	0.210 ± 0.012	$Na_2CO_3 \cdot H_2O$
	70.4	0.146 ± 0.008	$Na_2CO_3 \cdot H_2O$
	76.0	0.0704 ± 0.0044	$Na_2CO_3 \cdot H_2O$
45	0	48.30 ± 2.82	$Na_2CO_3 \cdot H_2O$
	8.10	37.50 ± 1.89	$Na_2CO_3 \cdot H_2O$
	16.6	30.70 ± 1.75	$Na_2CO_3 \cdot H_2O$
	25.4	17.114 ± 1.01	$Na_2CO_3 \cdot H_2O$
	44.8	1.460 ± 0.077	$Na_2CO_3 \cdot H_2O$
	64.9	0.232 ± 0.013	$Na_2CO_3 \cdot H_2O$
	70.4	0.150 ± 0.008	$Na_2CO_3 \cdot H_2O$
	76.0	0.0895 ± 0.0051	$Na_2CO_3 \cdot H_2O$
50	0	47.50 ± 2.56	$Na_2CO_3 \cdot H_2O$
	8.10	37.40 ± 1.81	$Na_2CO_3 \cdot H_2O$
	16.6	30.60 ± 1.62	$Na_2CO_3 \cdot H_2O$
	25.4	17.286 ± 1.01	$Na_2CO_3 \cdot H_2O$
	44.8	1.433 ± 0.068	$Na_2CO_3 \cdot H_2O$
	64.9	0.303 ± 0.019	$Na_2CO_3 \cdot H_2O$
	70.4	0.161 ± 0.008	$Na_2CO_3 \cdot H_2O$
	76.0	0.110 ± 0.005	$Na_2CO_3 \cdot H_2O$
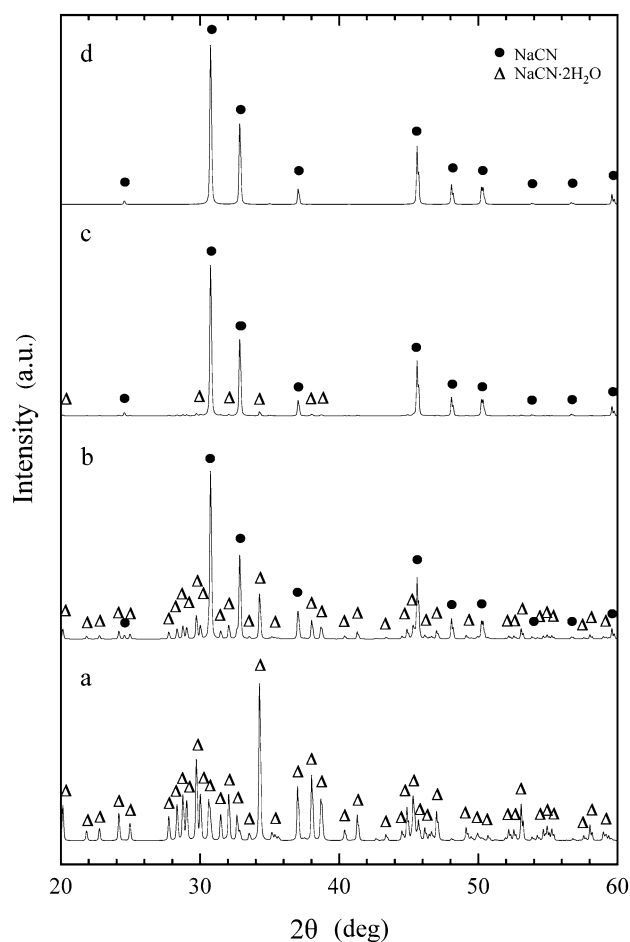
Fig. 2 XRD patterns for solid phases in NaCN–C_2H_5OH–H_2O ternary system at temperature of 27 °C in **a**, 31 °C in **b**, 35 °C in **c** and 40 °C in **d**. The content of ethanol in the solvent is 64.9 wt%

### 4.1.2 Selection of physical properties and determination of parameters

The correct choice of physical properties is a key part of the process simulation.

The eNRTL model is best known as a thermodynamic model for simulating the electrolyte equilibrium process in a mixed solvent system. The eNRTL model is a multivariate model for calculating the activity coefficient, which can be used not only in a water-soluble electrolyte system, but also in a mixed solvent–electrolyte system over a full range of electrolyte concentrations. This model can calculate the activity coefficient for ion species and molecular species in water soluble electrolyte systems and mixed solvent electrolyte systems.
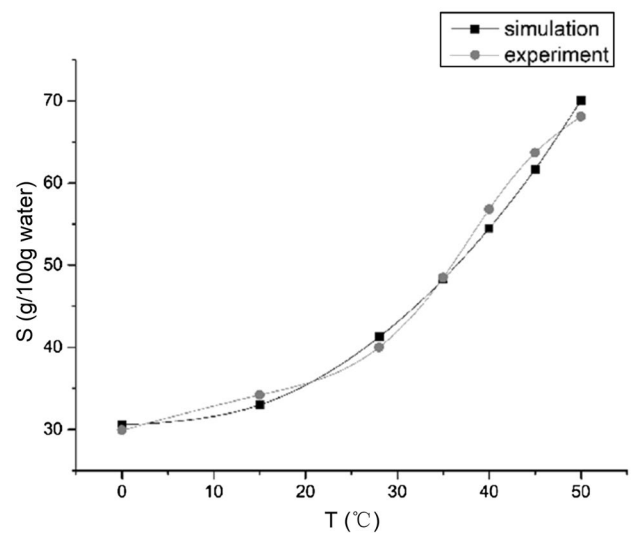
Therefore, in this paper, the eNRTL model was used to simulate the separation process of NaCN and Na_2CO_3 mixtures in a water–ethanol mixed solvent.

Table 5 Parameter values and standard deviations (SD) of the solubility relationship Eq. (2) of Na_2CO_3 according to mixed solvent composition

T (°C)	A	SD_A	B	SD_B	C	SD_C	D	SD_D	δ
25	33.173	0.861	−67.069	0.532	−48.682	0.984	107.607	1.464	0.98017
30	39.850	0.617	−92.421	0.608	−22.293	0.857	101.989	1.120	0.98739
35	47.646	0.349	−137.126	0.623	59.194	0.912	54.345	1.332	0.98697
40	48.444	0.552	−141.192	0.445	70.004	0.752	45.013	0.898	0.98376
45	48.709	0.663	−135.201	0.393	46.035	0.668	66.022	0.913	0.98289
50	47.994	0.431	−128.531	0.505	29.915	0.806	77.503	1.188	0.98191
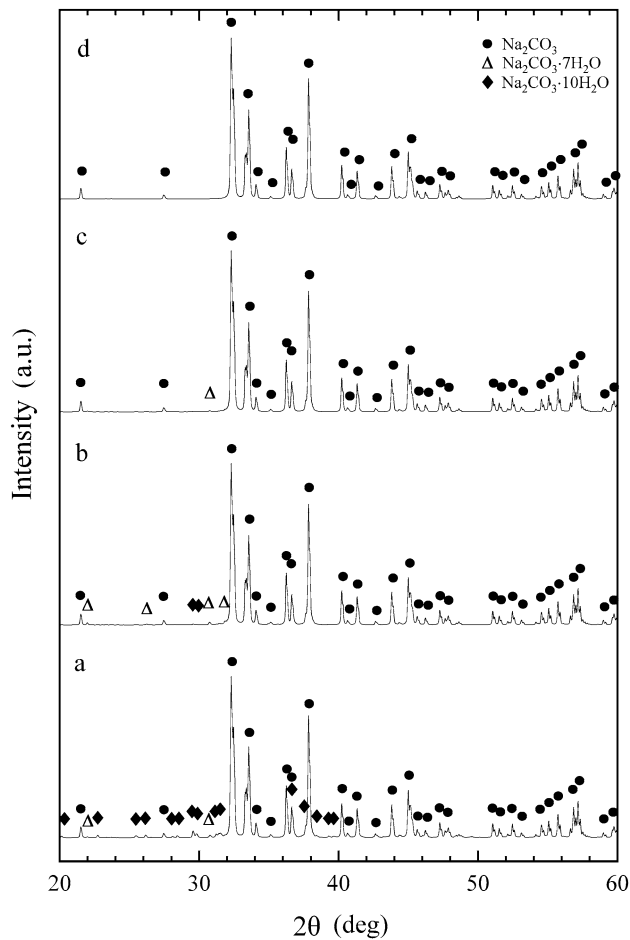
Fig. 3 XRD patterns for solid phases in Na_2CO_3–C_2H_5OH–H_2O ternary system at temperature of 25 °C in **a**, 30 °C in **b**, 35 °C in **c** and 40 °C in **d**. The content of ethanol in the solvent is 64.9 wt%

Fig. 4 NaCN solubility curve according to temperature in pure water

Table 6 H_2O–(Na^+, CN^-) molecule–electrolyte pair interaction parameter

Parameters	Component i	Component j	Value	Standard deviation
GMELCC/1	H_2O	(Na^+, CN^-)	31.695	0.063
GMELCC/1	(Na^+, CN^-)	H_2O	−9.455	0.025
GMELCD/1	H_2O	(Na^+, CN^-)	−7701.139	15.461
GMELCD/1	(Na^+, CN^-)	H_2O	1710.798	6.236
GMELCE/1	H_2O	(Na^+, CN^-)	−220.442	0.978
GMELCE/1	(Na^+, CN^-)	H_2O	69.014	0.252
GMELCN/1	H_2O	(Na^+, CN^-)	0.200	0.063

In Aspen PLUS, The eNRTL model parameters of a number of substances required for electrolytic activity coefficient calculation are already documented. However, there are many unknown parameters. So, Based on the measurement of the solubility of NaCN and Na_2CO_3 in the water–ethanol mixture, we have estimated the solvent molecules (water or ethanol)–electrolytes (NaCN and Na_2CO_3) pair interaction parameters by using data regression function of Aspen Plus.

## 4.2 Process simulation and determination of optimum conditions

4.2.1 Set initial input value

Table 10 shows the composition of the initial raw materials (mixture of NaCN and Na_2CO_3) and mixed solvents used in the process simulations. As shown in the table, the content

Table 7 C_2H_5OH–(Na^+, CN^-) molecule–electrolyte pair interaction parameter

Parameter	Component i	Component j	Value	Standard deviation
GMELCC/1	C_2H_5OH	(Na^+, CN^-)	6.547	0.886
GMELCC/1	(Na^+, CN^-)	C_2H_5OH	−1.282	0.540
GMELCD/1	C_2H_5OH	(Na^+, CN^-)	−632.518	3.358
GMELCD/1	(Na^+, CN^-)	C_2H_5OH	191.058	2.052
GMELCE/1	C_2H_5OH	(Na^+, CN^-)	−383.920	0.983
GMELCE/1	(Na^+, CN^-)	C_2H_5OH	−893.874	0.463
GMELCN/1	H_2O	(Na^+, CN^-)	0.200	0.886

Table 8 C_2H_5OH–(Na^+, CO_3^{2-}) molecule–electrolyte pair interaction parameter

Parameter	Component i	Component j	Value	Standard deviation
GMELCC/1	C_2H_5OH	(Na^+, CO_3^{2-})	11.282	0.309
GMELCC/1	(Na^+, CO_3^{2-})	C_2H_5OH	−0.207	0.864
GMELCD/1	C_2H_5OH	(Na^+, CO_3^{2-})	−1716.400	2.361
GMELCD/1	(Na^+, CO_3^{2-})	C_2H_5OH	222.794	6.557
GMELCE/1	C_2H_5OH	(Na^+, CO_3^{2-})	−618.760	0.473
GMELCE/1	(Na^+, CO_3^{2-})	C_2H_5OH	1048.327	1.854
GMELCN/1	C_2H_5OH	(Na^+, CO_3^{2-})	0.200	0.309
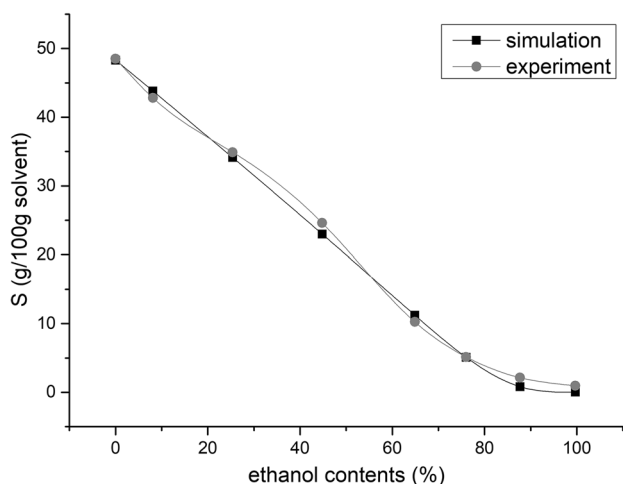
Fig. 5 Solubility curve of NaCN according to ethanol contents in water–ethanol mixture (T = 35 °C)

of NaCN in the initial raw material is 50 wt%, the content of ethanol in the mixed solvent is 70 wt%, and the ratio of the solid to liquid is 1:6.67.

The initial process conditions set in the unit operation models are shown in Table 11.
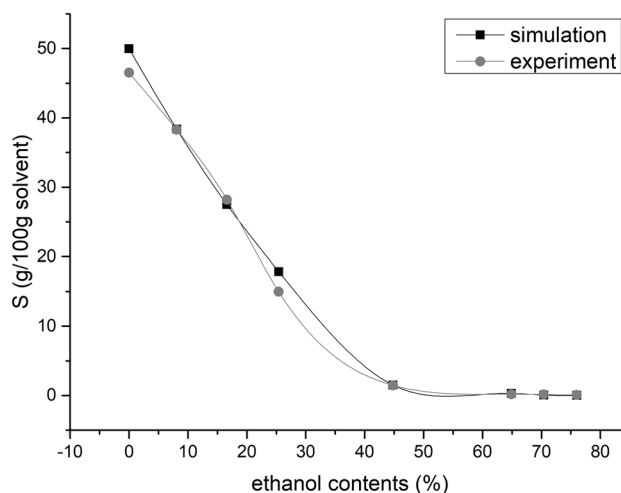
Fig. 6 Solubility curve of Na_2CO_3 according to ethanol contents in water–ethanol mixture (T = 35 °C)

4.2.2 Process simulation results and discussions

Table 12 shows the results of simulations using the initial raw materials and mixed solvent composition and process conditions. In Table 12, the material flow LEACHATE contains the content of each material component in equilibrium when the raw material is dissolved in the mixed solvent. The material flow Na_2CO_3 contains the content of the substance components contained in the precipitate taken from Centrifuge. The material flow FILTRATE contains the content of each substance component contained in the supernatant taken from the centrifuge. The content of each of the material components contained in the concentrate obtained by evaporation concentration in the crystallizer is included in the material flow TODRYER. Substance flow PRODUCT contains the content of each substance component in the final product obtained through the drying process.

As shown in Table 12, when the mixture of NaCN and Na_2CO_3 was dissolved in a mixed solvent of water and ethanol, NaCN was completely dissolved and Na_2CO_3 was almost completely precipitated as a $Na_2CO_3 \cdot H_2O$ (SALT2) crystal hydrate. Also, the purity of the separated Na_2CO_3 precipitate and the final NaCN product was very high, more than 99 wt%. From this, it can be seen that a mixed solvent can be used to effectively separate NaCN and Na_2CO_3.

4.2.3 Optimization of process conditions

In the process simulation, the purity and yield of NaCN products were investigated in various raw material conditions (NaCN contents are 20 wt%, 30 wt%, 40 wt%, 50 wt%,
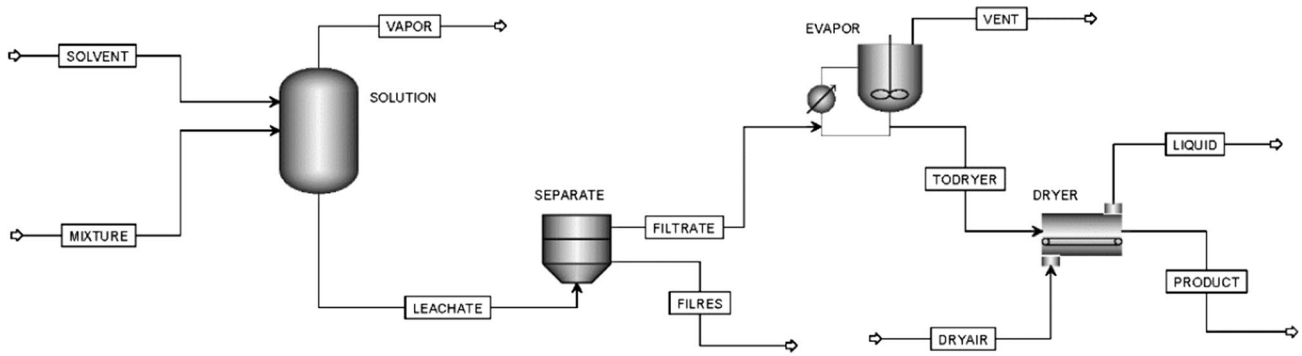
Fig. 7 The process diagram of separation of NaCN and Na_2CO_3 in a mixed solvent of water and ethanol

Table 9 Definition of components

ID	Type	Name	Formula
H_2O	Conventional	WATER	H_2O
C_2H_5OH	Conventional	ETHANOL	C_2H_5OH
Na_2CO_3	Conventional	SODIUM-CARBONATE	Na_2CO_3
NaCN	Conventional	SODIUM-CYANIDE	NaCN
H^+	Conventional	H^+	H^+
Na^+	Conventional	Na^+	Na^+
CO_2	Conventional	CARBON-DIOXIDE	CO_2
CN^-	Conventional	CN^-	CN^-
HCN	Conventional	HYDROGEN-CYANIDE	HCN
HCO_3^-	Conventional	HCO_3^-	HCO_3^-
OH^-	Conventional	OH^-	OH^-
CO_3^{2-}	Conventional	CO_3^{2-}	CO_3^{2-}
SODIU(S)	Solid	SODIUM-BICARBONATE	$NaHCO_3$
NaOH(S)	Solid	SODIUM-HYDROXIDE	NaOH
SALT1	Solid	SODIUM-CARBONATE	Na_2CO_3
SALT2	Solid	SODIUM-CARBONATE-MONOHYDRATE	$Na_2CO_3 \cdot H_2O$
SALT3	Solid	SODIUM-CARBONATE-HEPTAHYDRATE	$Na_2CO_3 \cdot 7H_2O$
SALT4	Solid	SODIUM-CARBONATE-DECAHYDRATE	$Na_2CO_3 \cdot 10H_2O$
NaCN(S)	Solid	SODIUM-CYANIDE	NaCN

Table 10 Composition of the initial raw materials and mixed solvents

Raw material (kg/h)		Mixed solvent (kg/h)		T (°C)	P (bar)
NaCN	Na_2CO_3	Water	Ethanol		
3	3	12	28	35	1

respectively) with varying solid–liquid ratio, solvent composition and dissolution temperature.

Table 11 Initial condition of process set in unit operation model block

No.	Unit operation model	Initial condition of process
1	SOLUTION (Flash2)	T = 35 °C, P = 1 bar
2	SEPARATE (CFuge)	Centrifugation mode Residual moisture content = 0.05
3	EVAPOR (Crystallizer)	Evaporation temperature = 50 °C Steam flow rate = 37.0 kg/h
4	DRYER (Dryer)	P = 1 bar, Residual moisture content = 0.05

Table 12 The mass flow rate of the components in material flow, which calculated by Aspen Plus simulation (kg/h)

Components	LEACHATE	FILRES (filtrated solid)	FILTRATE (liquid)	TODRYER (evaporated concentrate)	PRODUCT
T (°C)	35	35	35	50	20
P (bar)	1	1	1	0.105	1
Vapor phase fraction	0	0	0	0	0
Solid phase fraction	0.02	0.826	0	0.252	0.896
Total flow rate (kg/h)	46.1	3.694	42.406	5.406	3.088
H_2O	11.589	0.05	11.539	0.992	0.094
C_2H_5OH	28	0.121	27.879	1.428	0.009
H^+	Trace	Trace	Trace	Trace	Trace
Na^+	1.407	0.006	1.401	0.439	0.019
CO_3^{2-}	<0.001	Trace	<0.001	<0.001	<0.001
HCO_3^-	<0.001	Trace	<0.001	Trace	Trace
OH^-	0.001	Trace	0.001	0.003	0.003
CN^-	1.591	0.006	1.584	0.492	0.016
CO_2	Trace	Trace	Trace	Trace	Trace
HCN	0.001	Trace	0.001	Trace	Trace
NaCN(S)				2.052	2.948
SALT1					
SALT2	3.509	3.509			
SALT3					
SALT4					
pH	12.657	–	12.657	13.512	–

Table 13 Influence of solid–liquid ratio on NaCN separation efficiency

C_{NaCN} (%)	R	FILRES (filtrated residue)			PRODUCT			
		NaCN (kg)	$Na_2CO_3 \cdot H_2O$ (kg)	P (%)	NaCN (kg)	Na_2CO_3 (kg)	P (%)	Y (%)
50	1:5.00	0.728	3.510	82.8	2.283	0.001	>99	76.1
	1:5.50	0.480	3.510	88.0	2.511	0.001	>99	83.7
	1:6.00	0.232	3.510	93.8	2.760	0.001	>99	92.0
	1:6.50	0.012	3.509	>99	2.979	Trace	>99	99.4
	1:7.00	0.013	3.509	>99	2.979	Trace	>99	99.4
	1:8.00	0.011	3.509	>99	2.979	Trace	>99	99.4
40	1:4.00	0.675	4.212	86.2	1.712	0.001	>99	71.3
	1:4.50	0.427	4.212	90.8	1.970	0.001	>99	82.0
	1:5.00	0.178	4.212	95.9	2.218	0.002	>99	92.4
	1:5.50	0.016	4.212	>99	2.377	0.002	>99	99.0
	1:6.00	0.013	4.212	>99	2.381	0.002	>99	99.2
	1:7.00	0.012	4.211	>99	2.382	0.002	>99	99.2
30	1:3.00	0.620	4.914	88.8	1.178	0.001	>99	65.4
	1:3.50	0.372	4.914	92.9	1.424	0.001	>99	79.1
	1:4.00	0.123	4.914	97.5	1.673	0.001	>99	92.9
	1:4.50	0.017	4.914	>99	1.779	0.001	>99	98.8
	1:5.00	0.015	4.914	>99	1.780	0.002	>99	98.9
	1:5.50	0.013	4.914	>99	1.781	0.002	>99	98.9
20	1:2.50	0.314	5.616	94.7	0.884	0.001	>99	73.7
	1:3.00	0.067	5.616	98.8	1.130	0.001	>99	94.2
	1:3.50	0.017	5.616	>99	1.178	0.001	>99	98.2
	1:4.00	0.015	5.616	>99	1.180	0.001	>99	98.3
	1:4.50	0.013	5.616	>99	1.181	0.001	>99	98.4

- Influence of solid–liquid ratio

   The ethanol content in the mixed solvent was 70 wt%, and the dissolution temperature was fixed at 35 °C, and the separation efficiency of the raw material mixture was examined while varying the solid–liquid ratio. The results are shown in Table 13. Where C_{NaCN} is content of NaCN, R is the solid–liquid ratio, P is the purity, and Y is the yield.

   In the simulation, the total amount of raw material was fixed to 6 kg and the amount of solvent was changed. Other conditions are same as Tables 9 and 10.

   As shown in Table 13, as the solid–liquid ratio decreases, the purity of the NaCN product does not change, but the yield decreases. This is because, as the solid–liquid ratio decreases, NaCN does not completely dissolve in the mixed solvent and remains a precipitate with Na_2CO_3. On the other hand, as shown in Table 13, the optimum solid–liquid ratio decreases as the NaCN content in the raw material decreases. That is, when the content of cyanide in the raw material is 50 wt%, the optimum solid–liquid ratio is 1:6.5 and when the content is 40 wt%, it is 1:5.5. When the content of cyanide

is 30 wt%, the optimum solid–liquid ratio is 1:4.5 and when the content is 20 wt%, it is 1:3.5.

- Influence of Solvent Composition

   According to the composition of the raw material, the solid–liquid ratio is changed to the optimum solid–liquid ratio and the dissolution temperature is kept constant at 35 °C.

   Then, the results of examine the purity and yield of NaCN according to the content of ethanol in the mixed solvent is shown as Table 14. Where C_{NaCN} is the NaCN content in solution, $C_{ethanol}$ is content of Ethanol in mixed solvents, R is the solid–liquid ratio, P is the purity, and y is the yield. In the simulation, the amount of solid raw material was kept constant and only the mixed solvent content was changed. Other conditions are the same as above. As shown in Table 14, it can be seen that as the ethanol content in the solvent decreases, the purity of the NaCN product decreases, and when the ethanol content increases, the NaCN yield decreases sharply. This is because the low ethanol content does not cause a significant difference in solubility between the two electrolytes, so the product contains a large

Table 14 Effect of solvent composition on separation efficiency of NaCN

C_{NaCN} and R	$C_{ethanol}$ (wt%)	FILRES (filtrated residue)			PRODUCT			
		NaCN (kg)	$Na_2CO_3 \cdot H_2O$ (kg)	P (%)	NaCN (kg)	$Na_2CO_3 \cdot nH_2O$ (kg)	P (%)	Y (%)
50%, 1:6.5	35	0.010	2.628	99	2.960	0.877 ($n=7$)	77.1	98.6
	40	0.013	3.104	>99	2.960	0.713 (n=7)	80.5	98.6
	50	0.013	3.446	>99	2.967	0.091 (n=7)	97.0	98.9
	60	0.013	3.503	>99	2.974	0.006 ($n=1$)	>99	99.1
	70	0.012	3.509	>99	2.979	Trace	>99	99.4
	80	1.921	3.510	64.6	1.076	Trace	>99	35.9
40% 1:5.5	35	0.011	3.432	>99	2.361	0.778	75.2	98.4
	40	0.013	3.853	>99	2.360	0.356	86.9	98.3
	50	0.015	4.157	>99	2.366	0.079 (n=7)	96.7	98.6
	60	0.015	4.207	>99	2.374	0.004 (n=1)	>99	98.9
	70	0.016	4.212	>99	2.377	0.002	>99	99.0
	80	1.547	4.212	73.1	0.851	Trace	>99	35.4
30% 1:4.5	35	0.013	4.230	>99	1.762	0.681	72.1	97.9
	40	0.017	4.602	>99	1.763	0.546	76.4	98.0
	50	0.017	4.868	>99	1.769	0.064 (n=7)	96.5	98.3
	60	0.017	4.910	>99	1.775	0.003	>99	98.6
	70	0.017	4.914	>99	1.779	0.001	>99	98.8
	80	1.169	4.914	80.8	0.629	Trace	>99	34.9
20% 1:3.5	35	0.015	5.020	>99	1.164	0.595	66.2	97.0
	40	0.015	5.345	>99	1.167	0.473	71.1	97.2
	50	0.017	5.578	>99	1.175	0.045	96.5	97.9
	60	0.017	5.613	>99	1.177	0.002	>99	98.1
	70	0.017	5.616	>99	1.178	0.001	>99	98.2
	80	0.788	5.616		0.413	Trace	>99	34.4

Table 15 Influence of dissolution temperature on separation efficiency of NaCN products

C_{NaCN} and R	T (°C)	FILRES (filtrated residue)			PRODUCT			
		NaCN (kg)	$Na_2CO_3 \cdot H_2O$ (kg)	P (%)	NaCN (kg)	$Na_2CO_3 \cdot nH_2O$ (kg)	P (%)	Y (%)
50%, 1:6.5	25	1.353	3.510	72.2	1.642	0.001	>99	54.7
	30	0.932	3.510	79.0	2.060	0.001	>99	68.7
	35	0.012	3.509	>99	2.979	Trace	>99	99.4
	40	0.012	3.509	>99	2.979	Trace	>99	99.4
40%, 1:5.5	25	1.170	4.212	78.3	1.224	0.001	>99	51.0
	30	0.849	4.212	83.2	1.546	0.001	>99	64.4
	35	0.016	4.212	>99	2.377	0.002	>99	99.0
	40	0.015	4.211	>99	2.379	0.002	>99	99.1
30%, 1:4.5	25	0.857	4.914	85.1	0.939	0.001	>99	52.2
	30	0.607	4.914	89.0	1.188	0.001	>99	66.6
	35	0.017	4.914	>99	1.779	0.001	>99	98.8
	40	0.017	4.913	>99	1.779	0.002	>99	98.8
20%, 1:3.5	25	0.540	5.616	91.2	0.655	0.001	>99	54.6
	30	0.361	5.616	94.0	0.835	0.001	>99	69.6
	35	0.017	5.616	>99	1.178	0.001	>99	98.2
	40	0.017	5.615	>99	1.179	0.001	>99	98.3

amount of Na_2CO_3. And, when the ethanol content is too high, the solubility of NaCN is drastically lowered so that a large amount of NaCN is not dissolved and remains as a precipitate. As shown in Table 14, reasonable solvent composition is when the ethanol content of 60–70 wt%.

- Influence of dissolution temperature

According to the composition of the raw materials, the optimum mixing ratio was set as the solid–liquid ratio, and the ethanol content was fixed to 70 wt% in the mixed solvent. Then, the purity and deposition rate of the NaCN product were examined while varying the dissolution temperature. The results are shown in Table 15. As can be seen from Table 15, the lowering of the dissolution temperature leads to a lower yield of NaCN. This is because when the temperature is lowered, the solubility of NaCN is lowered and a part of NaCN precipitates without being dissolved in the mixed solvent. From this, the dissolution temperature should be raised to 35 °C or higher in order to increase the yield of NaCN. However, if the temperature is excessively high, the hydrolysis of NaCN will be accelerated, which will also affect the yield. Therefore, the most reasonable dissolution temperature is 35 °C.

Thus, the most reasonable process conditions for separating and purifying the mixture of NaCN and Na_2CO_3 by using a water–ethanol mixed solvent from the Aspen Plus simulation are described.

5 Conclusion

The solubility of NaCN and Sodium Na_2CO_3 in the water–ethanol mixture was determined through experiments and the relationship between the solubility of NaCN/Na_2CO_3 and the solvent composition are led. And the solvent molecular-electrolyte pair interaction parameters of eNRTL model were estimated by using the data regression function of Aspen Plus software from solubility data of NaCN and Na_2CO_3 in water–ethanol mixed solvent.

The process simulation for separation and purification of NaCN and Na_2CO_3 in water–ethanol mixed solvent was carried out by using Aspen Plus software. During the simulation, electrolyte equilibrium system in water–ethanol mixed solvent was observed by using eNRTL model property method, and the influence of several factors on the separation efficiency of NaCN was examined.

Based on the experimental results, when the content of cyanide in the raw material is 20–50 wt%, the optimum solid–liquid ratio is 1:3.5–1:6.5. Also, the concentration of ethanol in mixed solvents most suitable for NaCN separation is 60–70 wt%, most reasonable dissolution temperature is 35 °C.

Compliance with ethical standards

Conflict of interest The authors declare that they have no conflict of interests

References

1. Singhal S, Jain SL, Sain B (2010) Heterogeneously catalyzed oxidative cyanation of tertiary amines with sodium cyanide/hydrogen peroxide using polymer-supported iron(II) phthalocyanines as catalyst. Adv Synth Catal 352:1338–1344. https://doi.org/10.1002/adsc.201000007

2. Murahashi SI, Komiya N, Terai H, Nakae T (2003) Aerobic ruthenium-catalyzed oxidative cyanation of tertiary amines with sodium cyanide. J Am Chem Soc 125:15312–15313. https://doi.org/10.1021/ja0390303

3. Murahashi S-I, Komiya N, Terai H (2005) Ruthenium-catalyzed oxidative cyanation of tertiary amines with hydrogen peroxide and sodium cyanide. Angew Chem 117:7091–7093. https://doi.org/10.1002/ange.200501496

4. Murahashi SI, Nakae T, Terai H, Komiya N (2008) Ruthenium-catalyzed oxidative cyanation of tertiary amines with molecular oxygen or hydrogen peroxide and sodium cyanide: Sp3 C-H bond activation and carbon-carbon bond formation. J Am Chem Soc 130:11005–11012. https://doi.org/10.1021/ja8017362

5. Leisner P, Zanella C, Belov I et al (2017) Control of silver throwing power by pulse reverse electroplating. Trans Inst Met Finish 95:25–30. https://doi.org/10.1080/00202967.2017.1260895

6. Pan R, Tong M, Li J, et al. Preparation and purification of hydrogen cyanide, involves preheating ammonia gas, mixing with inert gas and compressed air, entering mixture into tube furnace from methanol feed nozzle, vaporizing methanol, and mixing with methanol. CN106745066-A

7. Lv S, Han Y, Wen X, et al. Purification of gold-extracting cyanide fluid involves adding cyanide fluid with sodium magnesium salt of xanthogenate, conducting ion-exchange reaction to form xanthate deposit, and separating cyanide fluid from precipitate. CN101186374-A

8. Cui RF, Hu MC, Jin LH et al (2007) Activity coefficients of rubidium chloride and cesium chloride in methanol-water mixtures and a comparative study of Pitzer and Pitzer-Simonson-Clegg models (298.15 K). Fluid Phase Equilib 251:137–144. https://doi.org/10.1016/j.fluid.2006.11.016

9. Wang P, Anderko A, Young RD (2002) A speciation-based model for mixed-solvent electrolyte systems. Fluid Phase Equilib 203:141–176. https://doi.org/10.1016/S0378-3812(02)00178-4

10. Liu C, Tang G, Ding H et al (2015) Determination of the solubility and thermodynamic properties of wedelolactone in a binary solvent of ethanol and water. Fluid Phase Equilib 385:139–146. https://doi.org/10.1016/J.FLUID.2014.10.031

11. Long B, Zhao D, Liu W (2012) Thermodynamics studies on the solubility of inorganic salt in organic solvents: application to KI in organic solvents and water-ethanol mixtures. Ind Eng Chem Res 51:9456–9467. https://doi.org/10.1021/ie301000b

12. Chen CC (1980) Computer simulation of chemical processes with electrolytes. PhD thesis, Massachusetts Institute of Technology. http://dspace.mit.edu/handle/1721.1/15864

13. Renon H, Prausnitz JM (1968) Local compositions in thermodynamic excess functions for liquid mixtures. AICHE J 14:135–144. https://doi.org/10.1002/aic.690140124

14. Chen CC, Song Y (2004) Solubility modeling with a nonrandom two-liquid segment activity coefficient model. Ind Eng Chem Res 43:8354–8362. https://doi.org/10.1021/ie049463u

15. Bollas GM, Chen CC, Barton PI (2008) Refined electrolyte-NRTL model: activity coefficient expressions for application to multi-electrolyte systems. AICHE J 54:1608–1624. https://doi.org/10.1002/aic.11485

16. Wang W, Zeng D, Yin X, Chen Q (2012) Prediction and measurement of gypsum solubility in the systems $CaSO_4$ + $HMSO_4$ + H_2SO_4 + H_2O (HM = Cu, Zn, Ni, Mn) at 298.15 K. Ind Eng Chem Res 51:5124–5134. https://doi.org/10.1021/ie201721m

17. Wang W, Zeng D, Wang J et al (2014) Experimental determination and modeling of the solubility of $CaSO_4$ $2H_2O$ and $CaSO_4$ in the quaternary system $CaSO_4$ + $MgSO_4$ + H_2SO_4 + H_2O. Ind Eng Chem Res 53:12839–12847. https://doi.org/10.1021/ie5021365

18. Cavalaglio G, Coccia V, Cotana F et al (2018) Energy from poultry waste: an Aspen Plus-based approach to the thermo-chemical processes. Waste Manag 73:496–503. https://doi.org/10.1016/J.WASMAN.2017.05.037

19. Puig-Gamero M, Argudo-Santamaria J, Valverde JL et al (2018) Three integrated process simulation using Aspen Plus®: pine gasification, syngas cleaning and methanol synthesis. Energy Convers Manag 177:416–427. https://doi.org/10.1016/J.ENCONMAN.2018.09.088

20. Larbi F, García A, del Valle LJ et al (2018) Simulation basis for a techno-economic evaluation of chitin nanomaterials production process using Aspen Plus® software. Data Brief 20:1556–1560. https://doi.org/10.1016/J.DIB.2018.08.130

Publisher's Note Springer Nature remains neutral with regard to jurisdictional claims in published maps and institutional affiliations.